

Instantaneous movement of krill swarms in the Antarctic Circumpolar Current

Geraint A. Tarling* and Sally E. Thorpe

British Antarctic Survey, Natural Environment Research Council, Cambridge, United Kingdom

Abstract

Antarctic krill are known to have strong swimming capabilities, but direct observations of the speed and direction of krill-swarm movement within their natural environment are rare. We identified and examined 4060 swarms within the main flow of the Antarctic Circumpolar Current (Scotia Sea) using a combination of an EK60 echosounder, a 153.6 kHz acoustic Doppler current profiler, and ground-truthing nets. Net displacement magnitude (m) and net angle of deviation (d) were determined by vector subtraction from the background flow immediately below them. Values were compared against control data sets in which swarms were absent. With greater background flow, m became increasingly lower than predicted, which suggests that drag influences swarm movement. The characteristics of the flow regime influenced swarm behavior, given that both m and d varied according to the direction of background flow. Furthermore, multiple-regression analysis indicated that swarm area, the vicinity of the sea-ice edge, and salinity had a significant influence on m , with levels of displacement being greatest in larger swarms and in low-salinity regions close to the ice edge. The ice edge is a key environment for Antarctic krill and swarm behavior may assist in retaining this location. Only fluorescence was found to have a significant influence on d , with deviations being greatest in regions of highest fluorescence. This agrees with laboratory observations of krill turning more frequently within food patches. We demonstrate that it is possible to measure instantaneous movement patterns in Antarctic krill swarms and, at large scales, these movements are consistent with current understanding of responses of krill to local stimuli such as sea-ice and patches of food.

Swarms of Antarctic krill form some of the highest concentrations of animal biomass found in any of the world's ocean, reaching densities of up to 2 million tons over an area of 100 km² (Nowacek et al. 2011). Krill swarm formations vary enormously, encompassing layers (Watkins and Murray 1998), schools (Hamner and Hamner 2000), and loosely packed aggregations of varying dimensions (Tarling et al. 2009). This variation between swarms may reflect differing physiological attributes of the individuals within them, with, for instance, feeding individuals adopting differing formations from those searching for food (Mauchline 1980; Hamner and Hamner 2000). Likewise, reproduction and molting may influence both swarm structure and vertical location in the water column (Tarling et al. 1999; Tarling 2003). External factors are also likely to play a role, with predation threat and availability of oxygen limiting the ratio of swarm volume and surface area to within certain bounds (Kils 1979; Brierley and Cox 2010) and advective forces further affecting length-to-thickness ratios and maximum swarm length (Zhou and Dorland 2004).

Swarming is a common behavioral trait in pelagic marine organisms that can improve fitness through reducing predation and increasing foraging success (Foster et al. 2001). Social interaction within swarms can also lead to the more effective sampling of patchy environments and improved taxis along gradients of, for instance, food or temperature (Grunbaum 1998). A further potential benefit is a decrease in the cost of swimming (Ritz 2000; Ritz et al. 2011). Yen et al. (2003) and Patria and Wiese (2004) identified vortices in the wake of euphausiids with upward- and forward-directed components that may assist the

propulsion of neighboring individuals. Aggregations may be structured to allow individuals to sense the hydrodynamic cues of neighboring krill and to position themselves so that they obtain maximum hydrodynamic benefit from their neighbors (Catton et al. 2011). Nevertheless, the energetic benefits of group swimming have proven to be difficult to measure experimentally and it has not yet been possible to scale up the hydrodynamic processes acting at an interindividual level to those operating at the level of the swarm (Swadling et al. 2005).

Much of our understanding of Antarctic krill swarm structure has come from studies carried out within inshore waters, where swarms can be tracked and their various properties monitored (Hamner et al. 1983; Strand and Hamner 1990; Hamner and Hamner 2000). For such studies to be successful, rates of advection must be generally low so that the swarms remain within the study area for repeated measurements. However, such environments represent a minor part of the total krill habitat, given that 87% of krill are found more than 200 km offshore (Aktinson et al. 2008). The open Southern Ocean contains some of the strongest currents of any ocean, with average surface geostrophic current magnitudes of about 16 cm s⁻¹ in Drake Passage, increasing to 50 cm s⁻¹ in frontal jets (Cunningham and Pavic 2007). Taking ageostrophic motion into account, surface current speeds can reach maxima of the order of 100 cm s⁻¹ (Smith et al. 2010). It is within this physical context that swarms of krill spend the majority of their time.

The response of aggregations to physical forcing is directly related to the swimming and behavioral capabilities of the individuals within them (McManus and Woodson 2012). Antarctic krill are among the largest euphausiid species, with an ability to maintain swimming speeds of up

* Corresponding author: gant@bas.ac.uk

to 15 cm s^{-1} without increasing metabolic rate (Kils 1981). Their individual capabilities may therefore be sufficient to maintain control over their location within highly advective environments. Furthermore, such prolific swimming capabilities may be vital to maintaining swarm coherence in the face of powerful dispersive forces (Zhou and Dorland 2004). Indeed, the capabilities of Antarctic krill swarms to maintain their integrity and oppose strong flows have been recognized for some time, with Hardy and Gunther (1935) reporting a swarm of krill swimming into a current for several hours at a speed of 17 cm s^{-1} , while, from in situ observations of krill swarms, Hamner (1984) reported that sustained speeds of 20 cm s^{-1} were “not unusual.”

At large oceanic scales, it is apparent that the distribution of Antarctic krill within the Antarctic Circumpolar Current is far from random. Atkinson et al. (2004) calculated that 50% to 70% of the total stock were within the sector 10° to 80°W . By contrast, other zooplankters show much more even circumpolar distributions (Atkinson et al. 2008). The pattern suggests that krill are able to influence their large-scale distribution through active swimming, of which most other zooplankters are incapable. Nevertheless, how krill swarms interact with prevailing advective forces to affect their pattern of distribution is far from clear. Models of krill horizontal migration have mainly taken a passive-particle transport approach (Hofmann et al. 1998; Fach and Klinck 2006) with modifications for vertical migration or association with sea-ice (Thorpe et al. 2007). The level of fit to observed distribution patterns could be improved through including further parameterizations on the responsiveness of swarms to their environment, particularly with respect to horizontal movement. However, such improvements are constrained by the fact that there is little or no direct evidence of swarms showing any taxis along clines of temperature, productivity, or sea-ice edges.

The lack of parameterizations of swarm movement reflects the difficulty of obtaining direct measurements. One approach is to track a swarm, as achieved by Clark and Morris (1983) and Nowacek et al. (2011). This allows the changing movement of the swarm to be monitored as both internal and external factors alter over space and time. However, in a highly advective open-ocean environment, this may mean tracking a swarm moving at above 20 cm s^{-1} , which becomes difficult to achieve on a single sampling vessel. Furthermore, the wider context of how the studied swarm is behaving relative to the wider population of krill swarms is unknown. An alternative is to measure the movement of many swarms instantaneously relative to the background flow. This provides a more comprehensive census of the swarms within an identified study area, even if the temporal evolution of movement within any one swarm is unknown. A further advantage is that a potentially large number of swarms may be observed across a wide range of environmental settings and encompass krill in a variety of internal physiological states, so allowing a comprehensive investigation of the potential influences on active swarm movement.

Acoustic Doppler current profilers (ADCPs) were principally designed for measuring ocean current profiles

but have become increasingly recognized as being capable of resolving biologically relevant information (Flagg and Smith 1989). The instrument uses Doppler shift to measure the instantaneous movement of particles in the water column as a proxy for the movement of the water body itself. Accuracy of results depends on the assumption that all resolved particles move passively, but measurements become biased if actively moving particles dominate the ensonified region. Numerous studies have shown that diel vertical migrations by zooplankton and micronekton (small fishes, shrimps, and squids) affect estimates of vertical velocity obtained by ADCPs, particularly near times of ascent in the evening and descent in the morning (Plueddemann and Pinkel 1989; Tarling et al. 2001). During migration, the speed of vertical migrators is generally a lot higher than vertical velocities generated by physical processes, so the biological signal is easily distinguishable. In the horizontal plane, instances of detecting such bias is more difficult given that horizontal velocities are generally at least an order of magnitude greater and much closer to the swimming speeds of pelagic organisms. Nevertheless, Demer et al. (2000) demonstrated that the velocities of fish schools in the horizontal plane were resolvable when a school was sufficiently large and moving in a homogenous manner at a speed greater than the level of precision of the ADCP. Furthermore, enough measurements of both the swarm and the surrounding background must be made to reduce measurement error.

Despite the difficulties in making direct measurements of swarm movement, such information is vital to effective management of krill stocks and the requirement to understand how stocks may move between major fishing regions (Hill et al. 2009). In this study, we measure the instantaneous movement of krill swarms across the Scotia Sea using acoustic information obtained through a combination of standard echosounder instrumentation and a vessel-mounted ADCP. The fact that more than 30% of the circumpolar population of krill is found in this sector of the Southern Ocean (Atkinson et al. 2008) makes it suited to a study of this type, since swarms are numerous and encompass a range of swarm types (Tarling et al. 2009). We analyze the data with two major aims: (1) to resolve the trajectory of swarms relative to the background flow to identify any offsets and (2) to identify any internal or external factors that may influence the relative movement of swarms within flows, particularly with regard to the parameterization of migration trajectories of swarms in the open ocean. Overall, this study works toward predicting how swarms move in the open ocean.

Methods

A survey was carried out by the R/V *James Clark Ross* between 09 January and 16 February 2003 within the Scotia Sea sector of the Southern Ocean. The survey encompassed eight transects within an area of around 30° longitude (1700 km) and 10° latitude (1100 km ; Tarling et al. 2009; Fig. 1A). The majority of transects were transited at speeds of $9\text{--}18 \text{ km h}^{-1}$. Transect paths crossed a number of oceanographic features such as fronts and eddies. Acoustic

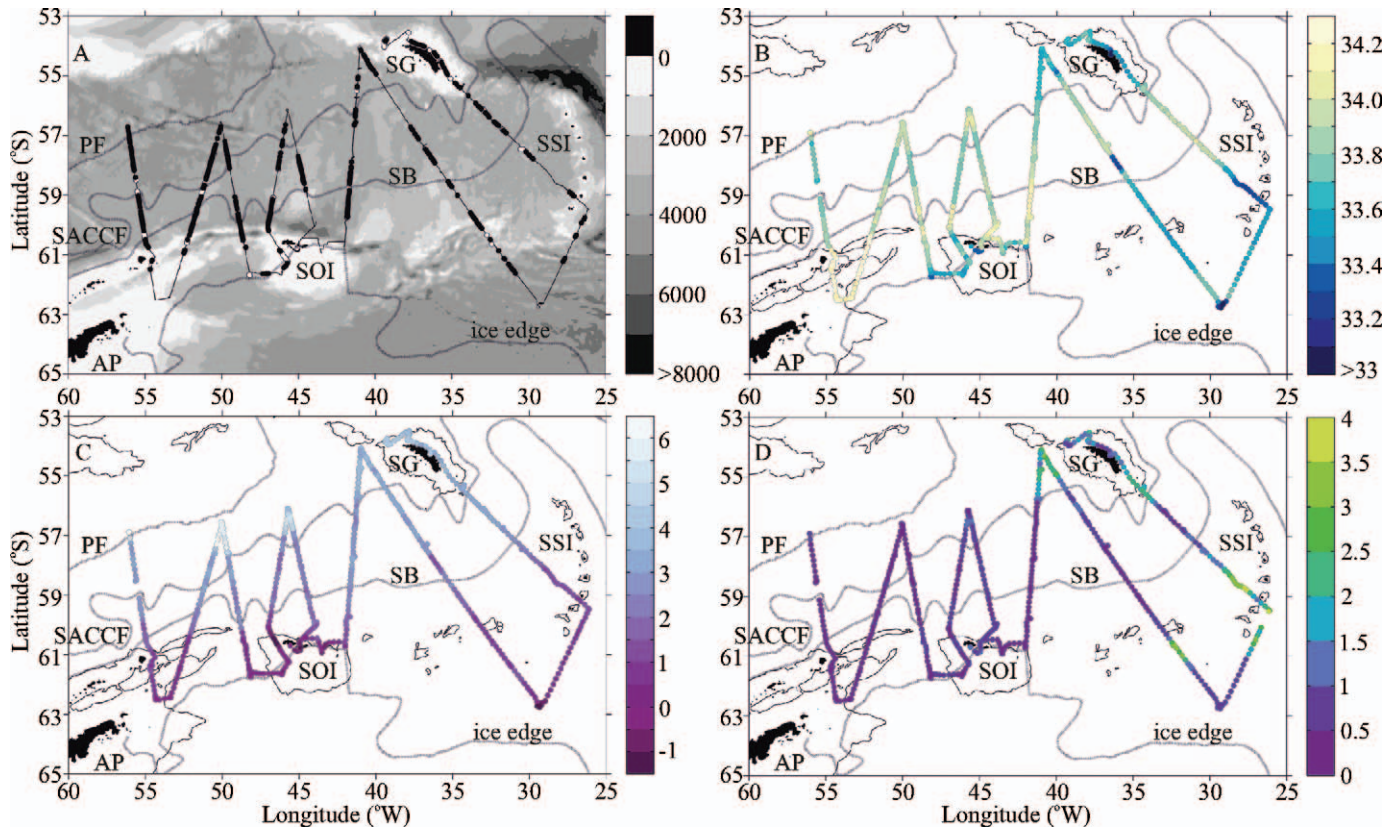


Fig. 1. (A) Cruise track along which swarm identification and tracking was performed. The locations of all swarms identified during the cruise are marked with circles; those marking swarms excluded from the factorial regression analysis are filled white. Bathymetry is shaded in 1000 m intervals. The location of land masses and climatological mean positions of water-mass fronts are indicated: Antarctic Peninsula (AP), South Georgia (SG), South Orkney Islands (SOI), South Sandwich Islands (SSI), Polar Front (PF; Moore et al., 1999), Southern ACC Front (SACCF, Thorpe et al. 2002), and southern boundary of the ACC (SB; Orsi et al., 1995). The ice edge represents the limit of 15% sea-ice concentration at the time of the cruise (Comiso 2000; updated 2012). For the purpose of visualization, the monthly mean January and February 2003 ice edges were merged at the cruise track longitude occupied on 27 January 2003 (41.85°W). (B) Along-track surface salinity values and (C) along-track surface temperature (°C) values measured by a thermosalinograph connected to an underway ocean-logger system. (D) Along-track surface fluorescence values (mg Chl *a* m⁻³) measured by a fluorometer connected to an underway ocean-logger system. (B–D) Measurements were carried out aboard the R/V *James Clark Ross* (January–February 2003) and were smoothed with a 60-min running mean.

data to detect krill swarms and measure their instantaneous movement were collected using a combination of a calibrated Simrad split-beam EK60 echosounder with 38 kHz and 120 kHz transducers and an RD Instruments narrow-band 153.6 kHz ship-mounted ADCP. Descriptions of how these instruments were set up and operated and the subsequent matching of the data streams are provided in more detail below. Net deployments were made intermittently along the transects from which krill population structure was determined and used for the parameterization of target strength models (*see below*).

Identification of krill swarms—The setup and operation of the EK60 echosounder as well as the postprocessing of echosounder data have already been described in detail in Tarling et al. (2009), so only a brief summary of these operations is provided here. The echosounder was calibrated in Stromness Bay (54°9.44'S, 36°41.99'W) on 17 February 2003 using a 60 mm copper sphere (*see Tarling et al. 2009 for calibrated transducer settings*). Raw acoustic

data from the 38 kHz and 120 kHz transducers were processed using Sonardata Echoview version 4.0 following the protocol of Hewitt et al. (2004), and with background noise levels subtracted (Watkins and Brierley 1996) and bad-data regions filtered out. A threshold of -70 dB at 120 kHz was set following Lawson et al. (2008). A swarm-detection algorithm was applied to the processed 120 kHz echogram data using Sonardata Echoview version 4.0 “School detection module,” which uses a shoal analysis and patch estimation system algorithm (Coetzee 2000) to identify swarm candidates according to preset criteria. In this instance, minimum total swarm length was set to 15 m, minimum distance between candidates 75 cm, minimum total swarm height 2 m, maximum horizontal linking distance 15 m, and maximum vertical linking distance 5 m.

After the swarm-detection process, both 38 and 120 kHz data were exported for interrogation by the $\Delta S_{V120-38}$ identification technique (CCAMLR 2005) to identify which swarms contained exclusively Antarctic krill. Minimum and maximum $S_{V120-38}$ values for different size ranges of

krill were identified from morphometric measurements on samples obtained from accompanying net samples (Tarling et al. 2009). The parameters were fed into a simplified stochastic distorted wave-borne approximation (SDWBA) target strength model (McGehee et al. 1998; Demer and Conti 2003; Conti and Demer 2006), using fixed values for orientation of 11° (standard deviation = 4°) and a distribution drawn from 99% of the krill length frequencies estimated from a cumulative distribution function, binned into ranges recommended by Commission for the Conservation of Antarctic Marine Living Resources (CCAMLR 2005, table 3). The material properties of krill were based on those calculated for the CCAMLR synoptic survey in the Scotia Sea region at the same time of year as the present study (Conti and Demer 2006).

Once identified, the following physical properties for each swarm were extracted: (1) mean swarm thickness (m), (2) mean swarm length (m), (3) mean swarm area (m²), (4) the minimum distance to the next swarm (km), (5) packing concentration (individuals [ind.] m⁻³). Parameter 5 relies on the application of a target strength value that was set between -74.45 and -74.66 at 120 kHz, as determined from the SDWBA model (above).

Measurement of swarm movement—An RD Instruments narrow-band 153.6 kHz ship-mounted ADCP was used to collect underway measurements of current magnitude. The ADCP was in a “janus” configuration, i.e., with two beams looking forward and two looking back at an angle of 30° from vertical in 90° azimuth increments. The firmware version was 17.07, and the data acquisition software, RD Instruments version 2.48. The ensemble period was set to 2 min at a ping rate of 1 Hz, resulting in approximately 120 pings per ensemble. Depth bins were set to 8 m and the blank after transmit, 4 m. The center of the first bin was set to a depth of 18 m with a total of 64 depth bins being collected per ensemble. Random error in horizontal velocity was calculated at 1.19 cm s^{-1} . All measurements with % good values of less than 50 were screened out from any further analyses of krill swarm movement.

Determining background current baseline—Swarm movement can only be determined by first accounting for the background flow. We considered three methods of determining background flow using ADCP data, through using: (1) bins, at mean swarm depth, immediately before the front edge of a swarm, (2) bins immediately above a swarm, and (3) bins immediately below a swarm. In all cases, a single bin was chosen to represent background flow movement since this allowed all sizes of swarms to be measured on a similar basis. Simulation data sets were generated to identify which of the three methods had the greatest capacity to predict background flows within krill swarms. Locations (4988) were selected at random along the cruise track (the number equivalent to the total number of krill swarms identified during the survey). All locations containing krill swarms were rejected. For each of the remaining locations, swarms were simulated through randomly selecting swarm-depth and -length values from the observed distributions of these parameters (Table 1A)

and then using these to define the region of a “fake” swarm (denoted f as opposed to an observed swarm, denoted s). The background flow within this fake swarm was then predicted using methods 1 to 3 and compared with the true background flow within the fake swarm (henceforth, flows measured outside of the swarm area are denoted pre, and within the swarm area, obs, both with respect to fake swarms and real swarms).

Methods 2 and 3, of selecting bins immediately above or below the swarm, were found to have the best predictive capacity (Pearson product moment correlation, before: 0.881; below: 0.942; above: 0.949). However, there was a large amount of missing data in the above swarm data set, since the required depth of measurement was frequently above the upper depth range of the ADCP beams. The below swarm method (method 3) was therefore chosen to predict background movement of krill swarms.

Estimating net swarm movement—The matching of swarms to ADCP depth-time bins was performed through determining the time at which the start and midpoint of each swarm were observed on the echosounder charts and relating these back to the ADCP records. The maximum depth of the swarm was also noted. Vectors for the eastward and northward components of velocity (u and v respectively) from the center point of the swarm (obs) and from immediately below the swarm (pre) were extracted from the corresponding ADCP bins. Net swarm movement relative to background flow was then estimated through vector subtraction, as follows:

$$m = \sqrt{(u_{\text{pre}} - u_{\text{obs}})^2 + (v_{\text{pre}} - v_{\text{obs}})^2} \quad (1)$$

$$d = -(\text{atan2}[u_{\text{pre}}, v_{\text{pre}}] - \text{atan2}[u_{\text{obs}}, v_{\text{obs}}]) \quad (2)$$

where m is net displacement magnitude of swarm movement (cm s^{-1}), d is net angle of deviation of swarm movement, converted from radians to degrees ($-180^\circ < d < 180^\circ$), and

$$\text{atan2}(u, v) = 2 \arctan \frac{u}{v + \sqrt{u^2 + v^2}} \quad (3)$$

Equation 2 results in positive values denoting a counter-clockwise deviation from the background flow, and negative values, a clockwise deviation.

Relationships between the velocity magnitude within swarms (M_{obs}) and below swarms (M_{pre}) were also examined in both observed and fake swarms as a further means of characterizing interactions between swarms and the strength of the background flow, such that

$$M_{\text{obs}} = \sqrt{u_{\text{obs}}^2 + v_{\text{obs}}^2} \text{ and } M_{\text{pre}} = \sqrt{u_{\text{pre}}^2 + v_{\text{pre}}^2} \quad (4)$$

Data analysis—From an initial inventory of 4988 swarms, it was possible to perform the ADCP analyses on a total of 4060 swarms, after the exclusion of (1) bad ADCP data (i.e., % good of < 50), (2) swarms where it was not possible to obtain an ADCP measurement immediately

Table 1. Physical characteristics of Antarctic krill swarms encountered during the survey ($n=4988$).

	Depth (m)	Length (m)	Thickness (m)	Area (m ²)	Distance to next swarm (km)	Ind. m ⁻³
Mean	45.73	104.98	6.66	513.43	0.54	28.52
SD	39.99	411.89	7.33	4147.03	4.46	94.02
Median	33.98	41.04	4.25	55.07	0.11	8.38
25th percentile	23.40	25.40	2.39	25.18	0.05	5.97
75th percentile	50.24	77.12	7.97	159.74	0.23	16.60
Minimum	8.29	10.08	1.28	4.70	0.00	2.17
Maximum	295.58	18,293.78	94.96	132,798.12	222.33	2559.43

below because of the presence of other swarms, or (3) poor-quality ADCP data because of, e.g., changes to ship's speed. This data set was used for the comparison of M_{obs} and M_{pre} to identify interactions related to the strength of background flow. This data set was then subsequently divided according to the direction of the background flow such that each swarm was placed within one of four 90° sectors, which were southwest, southeast, northwest, and northeast. Other physical characteristics of swarms relevant to our study are listed in Table 1.

In a separate analysis, swarm movement was matched against a set of potential explanatory variables, which included the physical properties of the swarms themselves (*see above*) and also a set of external variables considered pertinent to the condition and behavior of krill (Table 2). Full details on the collection of these parameters are given in Tarling et al. (2009), but briefly, parameters were extracted from a combination of (1) station sampling using a SeaBird 911 conductivity–temperature–depth recorder containing a 12-position carousel water sampler with 10 liter Niskin bottles, (2) underway sampling via the ship's "ocean-logger" system, which comprised a thermo-salinograph and fluorometer connected to a nontoxic seawater supply pumped from 6.5 m below the water's surface, and (3) satellite observation, principally the U.S. Air Force Defense Meteorological Satellite Program special

sensor microwave imager passive microwave data provided by National Oceanic and Atmospheric Administration and National Centers for Environmental Prediction to locate the nearest ice edge. For those parameters measured at stations, a distance minimization algorithm was used to link them to respective swarms in the vicinity. We used some variables to represent others where strong relationships existed between them (e.g., underway fluorescence and surface chlorophyll *a* [Chl *a*]), since this reduced the number of variables and increased the efficiency of the analytical process. Limitations in the coverage of some parameters resulted in the analytical data set being restricted to 1886 swarms.

Best-subset analysis was implemented in Minitab version 15.1.0.0 (Minitab 2006) to identify any subsets of parameters with significant explanatory power toward observed variations in swarm movement. Best-subset analysis aims to achieve the best fit to observations with as few predictors as possible using the maximum R criterion. Evaluation of models was further assessed using the Mallows' Cp score, where a value that is close to the number of predictors plus the constant indicates that the model is relatively precise and unbiased in estimating the true regression coefficients and predicting future responses. The analysis was carried out with a total of 12 parameters as free predictor variables and either m or d as the response variable. Outputs from

Table 2. Biological and environmental parameters used in analyses, either as descriptors of swarm movement or as potential explanatory variables. ADCP, acoustic Doppler current profiler; GIS, geographic information system; GPS, global positioning system.

Variable	Descriptor or explanatory variable	Unit	Data source
Mean length	Swarm descriptor	m	Echosounder analysis
Mean thickness	Swarm descriptor	m	Echosounder analysis
Mean area	Swarm descriptor	m ²	Echosounder analysis
Distance to next swarm	Swarm descriptor	km	Echosounder analysis
Packing concentration	Swarm descriptor	ind. m ⁻³	Echosounder analysis
Net displacement magnitude (m)	Swarm descriptor	cm s ⁻¹	ADCP analysis
Net angle of deviation (d)	Swarm descriptor	°	ADCP analysis
Velocity magnitude of background flow (M_{pre})	External factor	cm s ⁻¹	ADCP analysis
Direction of background flow (D_{pre})	External factor	°	ADCP analysis
Surface temperature	External factor	°C	Ocean-logger
Surface salinity	External factor	Unitless	Ocean-logger
Underway surface fluorescence	External factor	mg m ⁻³	Ocean-logger
Photosynthetically active radiation (PAR)	External factor	μE m ⁻² s ⁻¹	Ocean-logger
Distance to nearest coast	External factor	km	GIS analysis
Bottom depth	External factor	m	GIS analysis
Distance to nearest ice edge	External factor	km	GIS analysis
Latitude	External factor	°	GPS recording

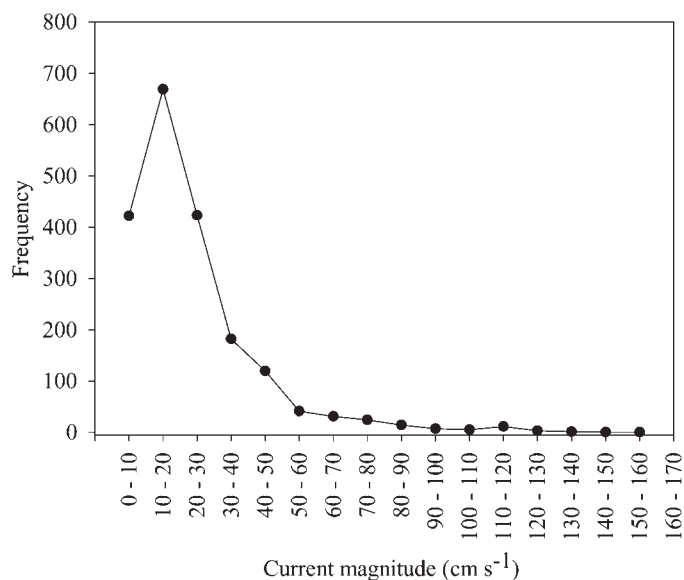


Fig. 2. Frequency distribution of velocity magnitudes (cm s^{-1}) across all swarm locations along the present cruise track.

the analysis were visualized as multiple regression plots to consider their explanatory power.

Results

Distribution of swarms within the flow-field—The majority of swarms (78%) were located in background flows of between 0 and 30 cm s^{-1} , with the greatest proportion (34%) occurring within flows of between 10 and 20 cm s^{-1} (Fig. 2). The direction of these flows was principally between north-northeast and east-southeast, although a minor southward component was also evident (Fig. 3).

Relationship to strength of background flow (M_{pre})—The best-fitting relationship between M_{pre} and M_{obs} was found to be linear regression, both for the observed swarm data set and the fake swarm data set (Fig. 4). A comparison of the respective regressions found both the slopes and elevations to be significantly different (slope: t -test, $t = 5.967$, degrees of freedom [df] = 6422, $p < 0.001$; intercept: t -test, $t = 5.814$, df = 6419, $p < 0.001$). The difference between $M_{obs,f}$ and $M_{obs,s}$ was 0.42 cm s^{-1} in background flows of 1 cm s^{-1} , increasing to 1.89 cm s^{-1} in background flows of 50 cm s^{-1} .

Relationship to direction of background flow—The relative movement of swarms was found to be dependent on the direction of the background flow (Table 3). There was no significant difference in m between the fake-swarm and the observed-swarm data sets in swarms within background flows heading southeast and northeast. However, m was significantly greater in swarms within northwest flows and significantly lower in swarms within southwest flows. A significant difference in d between fake and observed swarms occurred only in swarms located in flows heading northeast. The median deviation for swarms

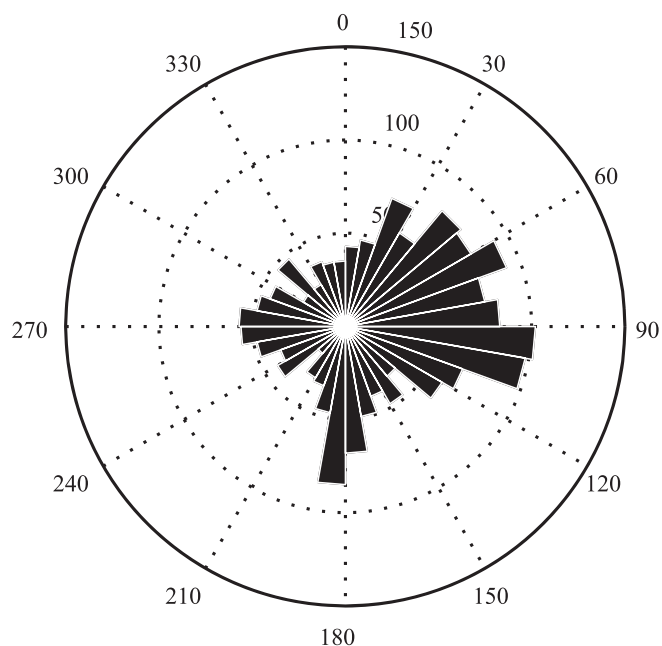


Fig. 3. Frequency distribution of the direction of the prevailing ocean flow ($^{\circ}$) across all swarm locations along the present cruise track.

found in those flows was 2.07° counterclockwise to the movement observed in fake swarms.

Predicting the net magnitude of swarm movement (m')—Log swarm area (m^2), salinity (unitless), and distance to nearest ice (km) were identified as the variables with the highest explanatory power with regard to variance in m (Table 4). The relationship with log swarm area was positive, meaning that, as swarms became larger, their displacement magnitudes were greater (Fig. 5). By contrast, the relationship with salinity and distance to ice was negative, meaning that swarms in high-salinity regions and farther from the ice were more likely to conform to the background flow, whereas those near the ice edge and within areas of low salinity were more likely to exhibit displacement from the background flow. The preferred model was as follows:

$$m' = 44.2 + 0.987 \log \text{swarm area} - 0.00191 \text{ distance to ice} - 1.14 \text{ salinity} \quad (5)$$

(ANOVA, $F_{1880} = 22.63$, $p < 0.0001$) where m' is predicted net magnitude of swarm movement, in cm s^{-1} .

The influence of each of the predictor variables on m' is further illustrated in Fig. 6. m' is plotted against log swarm area (m^2) with values for the other two parameters varying between their mean, minimum, and maximum levels. m' varied between 4.8 and 10 cm s^{-1} , with a median value of 7 cm s^{-1} . In conditions of high salinity, the tendency was for m' to decrease, by up to 0.5 cm s^{-1} , whereas lowering salinity increased m' by up to 0.8 cm s^{-1} . Distance to nearest ice had a similar level of influence, with values of m' varying by around $\pm 1 \text{ cm s}^{-1}$ within its range limits.

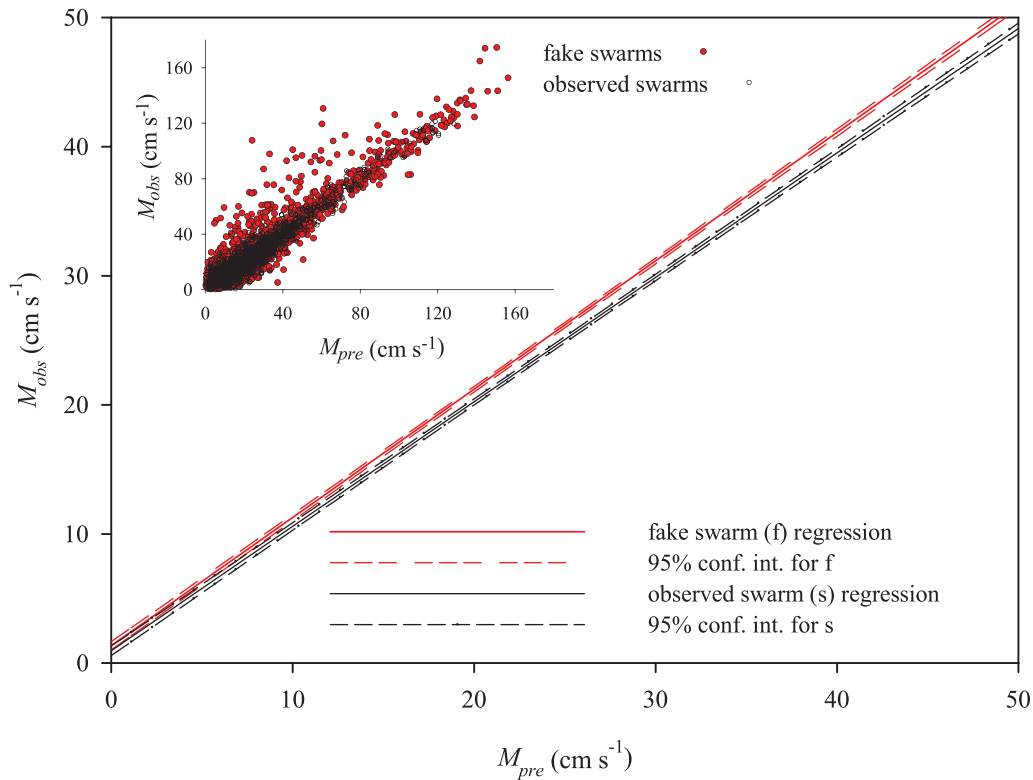


Fig. 4. Linear regressions of predicted against observed velocity magnitudes within swarms that were simulated (fake swarms, red lines) and directly observed (black lines). Dashed lines indicate 95% confidence intervals (conf. int.). Inset shows the individual data points to which the regressions were fitted.

In geographic terms, the model predicts that m' is highest (i.e., krill swarms show the greatest amount of displacement from background flow movement) in the vicinity of the Antarctic Peninsula and within Drake Passage, between 55° and 50°W , and also at the ice edge close to the South Orkneys (Fig. 7). Predicted values of m' in these regions were between 8 and 10 cm s^{-1} . Some of the lowest predicted values of m' were toward the Polar Front in the Drake Passage region and also in the vicinity of South Georgia, where values were typically between 5 and 7 cm s^{-1} .

Predictors of net direction of swarm movement (d')—Fluorescence ($\text{mg Chl } a\text{ m}^{-3}$), temperature ($^\circ\text{C}$), and latitude ($^\circ$) were identified as individual variables with the highest explanatory power toward variance in d (Table 5). Of these, only fluorescence was found to be a significant predictor of d

(Fig. 8). Therefore, the preferred model contained fluorescence as the only predictor variable, as follows:

$$d' = 2.89 - 4.36 \text{ fluorescence} \quad (6)$$

(ANOVA, $F_{1880} = 8.33$, $p = 0.004$) where d' is predicted net angle of deviation, in degrees.

Ninety percent of swarms occurred in levels of fluorescence of less than $1\text{ mg Chl } a\text{ m}^{-3}$, meaning that the value of d' was predicted to be $\pm 1.5^\circ$ (Fig. 9). For the 10% of swarms that occurred in higher levels of fluorescence, their value of d' was predicted to be increasingly negative, becoming less than -10° where fluorescence was above $3\text{ mg Chl } a\text{ m}^{-3}$. Therefore, the largest angles of deviation were predicted to occur at the highest levels of fluorescence, with a clockwise direction relative to the background flow.

Table 3. Median displacement vector (cm s^{-1}) and median angle of deviation ($^\circ$) in fake and observed swarms divided according to direction of background flow (divided into 90° quadrants). Symbols indicate significant deviation in observed swarms compared with fake swarm values. $*0.01 < p < 0.05$, $** p < 0.01$.

Direction of background flow	Median displacement vector (cm s^{-1})			Median angle of deviation ($^\circ$)		
	Fake swarms	Observed swarms	Observed–fake	Fake swarms	Observed swarms	Observed–fake
Southeast	5.94	6.02	0.08	-0.76	-0.31	0.45
Southwest	6.69	5.78**	-0.91	-0.56	0.21	0.77
Northwest	5.78	6.24*	0.46	-0.32	-0.94	-0.62
Northeast	5.88	5.88	0.00	-1.13	0.94*	2.07

Table 4. Best-fitting regression models constructed from the predictor variables specified in Table 2 and with m as the response variable. The table shows the two best models for each number of predictors up to a maximum of three predictor variables. Models are ranked according to a combination of the number of variables, R^2 , R^2 (adj) values (i.e., adjusted according to number of predictor variables in the model), Cp mallows (comparison of precision and bias in subsets of predictors relative to all predictors), and the value of S (the standard error of the regression representing the standard deviation of the residuals). The preferred model is indicated by **.

No. of variables	R^2	R^2 (adj)	Cp mallows	S	1	2	3	4	5	6	7	8	9	10	11	12	13
1	2.7	2.6	19.6	4.2146			X										
1	2.4	2.3	26.1	4.2218		X											
2	3.2	3.1	11.7	4.2048			X						X				
2	3.1	3.0	14.3	4.2076			X			X							
3**	3.5	3.3	8.0	4.1995			X						X		X		
3	3.5	3.3	8.9	4.2005			X					X	X				

1. Log swarm length (m). 2. Log thickness (m). 3. Log area (m²). 4. Log distance to next swarm (m). 5. Log packing concentration (ind. m⁻³). 6. Latitude (°). 7. Distance to coast (km). 8. Bottom depth (m). 9. Distance to ice (km). 10. Temperature (°C). 11. Salinity. 12. PAR ($\mu\text{E m}^{-2} \text{s}^{-1}$). 13. Fluorescence (mg Chl $a \text{ m}^{-3}$).

Geographically, the model predicts a greater deviation in the vicinity of South Georgia and also around the South Sandwich Islands, where d' was typically between -5° and -10° (Fig. 10). In the southwestern sector, close to the Antarctic Peninsula, there was a negligible amount of deviation from background flow.

Discussion

In this study we made measurements on 4060 positively identified krill swarms of at least 15 m in length and 2 m in vertical thickness. Net displacement magnitude had a coefficient of variation (CV) of 60.9% across all swarms, whereas the CV of the net angle of displacement was 17.6%. This variation between krill swarms is the result of a combination of both measurement error and biological variance. To account for measurement error, we compared the movements of krill swarms to levels of background shear in the water column. We selected data from the same part of the cruise track using the same dimensions and vertical distribution of the observed krill swarms but excluded data where swarms were present (i.e., a data set of fake swarms). Once measurement error had been accounted for, biological variance was examined through comparing the movement of swarms to behavioral and environmental parameters to identify significant explanatory factors. Although a large fraction of variance was not accounted for through these approaches, the analysis identified significant relationships between the movement of swarms and a number of both biological and environmental factors.

General patterns of swarm movement—Active vs. passive movement within the flow field: We found that the largest proportion of swarms were located in waters between 10 and 20 cm s⁻¹ where the main direction of flow was between north-northeast to east-southeast. Within these flows, the instantaneous movement of swarms exhibited a significant 2° counterclockwise deviation. Nevertheless, there was no difference found in the accompanying displacement magnitude, which probably reflects the fact that such deviation, although significant, is relatively small. Significant differences in displacement magnitude were

observed in swarms found within flows heading northwest and southwest. In the case of the former, the displacement magnitudes were greater than expected from passive particles whereas, in the latter, they were smaller than expected. This can be interpreted as swarms within northwest flows behaving to alter their trajectory, whereas swarms in southwest flows behave to conform to the flow.

The biogeographic distribution of Antarctic krill is known to be limited by the Polar Front (PF, Marr 1962) and is more abundant still south of the Southern Antarctic Circumpolar Front (SACCF, Ward et al. 2012). The PF and SACCF occur at much higher latitudes toward the west of the survey area compared with the east. For example, the PF is located at 58°S at 60°W (i.e., above the tip of the Antarctic Peninsula), whereas at 40°W, it is considerably north of South Georgia (54°S). This means that a particle traveling in a northwestward direction will cross gradients of increasing temperature and arrive at frontal boundaries far more rapidly than particles heading northeast. One interpretation of the above pattern of swarm movement is that it is an active avoidance of being displaced into unfavorable waters, closer to the PF, which would be sensed more locally through the gradient of temperature. Further supporting evidence is that swarms in southwestward flows show a significantly lower displacement than predicted, meaning that they are actively maintaining their direction and speed of movement in this direction. In effect, krill within these swarms are working against factors such as shear and small-scale turbulence that would otherwise alter their velocity and direction, as is the case in the fake swarms (i.e., swarm-sized regions of passive particles). Therefore, the swarms appear to work against flows in unfavorable directions, i.e., toward the PF, and to work with flows that help maintain them within Antarctic water masses.

Influence of drag: We found that the amount by which swarms were slower than background flow increased with increasing background velocity magnitudes. Regressions of predicted against observed flows were significantly different between the fake and observed krill swarm data sets, with the former producing a slope of 0.99 and the latter 0.96. This equates to the average krill swarm slowing at a rate of 0.03 cm s⁻¹ for every 1 cm s⁻¹ increase in background velocity.

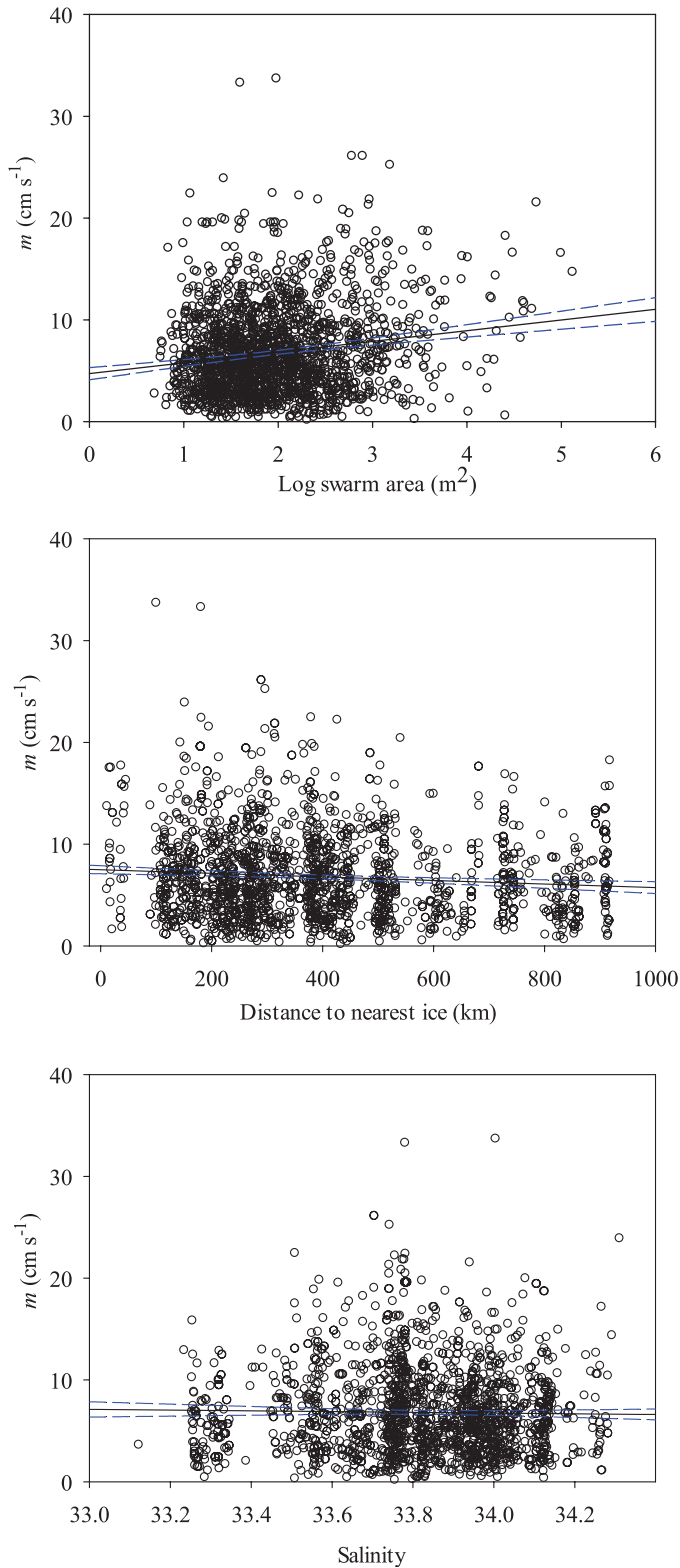


Fig. 5. Linear regression models fitted to m (cm s^{-1}) as the dependent variable and with either (A) log swarm area (m^2), (B) distance to nearest ice (km), or (C) salinity, as the independent variables, representing the three variables with the highest explanatory powers. Dashed lines represent 95% confidence intervals.

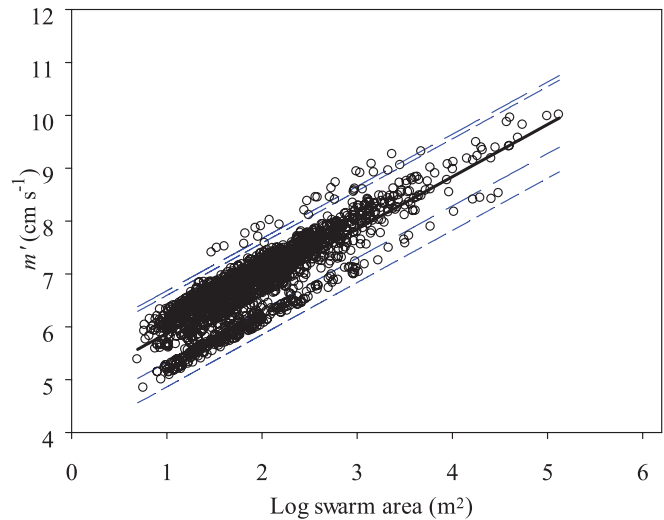


Fig. 6. Predicted response of m (cm s^{-1}) to log swarm area (m^2) at average levels of salinity and at a mean distance from the nearest ice (km). Short-dashed lines indicate the maximum and minimum influence of distance to nearest ice, long-dashed lines the maximum and minimum influence of salinity with the remaining variables being held at mean levels.

Such a slowing of an object while passing through a medium suggests the influence of drag. The drag force (F_D) is related to the density (ρ) of the medium in which the object is located, the planar area (A) perpendicular to the movement, and the velocity (V) of the object relative to the velocity of the medium and the drag coefficient (C_D) as follows:

$$F_D = C_D \frac{1}{2} \rho A V^2 \quad (7)$$

The drag coefficient depends on the size, shape, and weight of the object but it is usually associated with the extent to which the object is streamlined. Kils (1981) estimated the drag coefficient on individual krill held within a chamber at different planes to a prevailing flow. For a 57 mm (adult) krill, C_D was estimated to be 1.11 for a krill held at 90° to the prevailing flow and 0.31 for krill held at 0° to the prevailing flow. Antarctic krill have been observed to adopt a relatively horizontal orientation within school formation in both field and laboratory studies (Hamner and Hamner 2000; Catton et al. 2011), which would improve their drag coefficient and contribute to more energy-efficient swimming, as discussed above. Looser aggregations are likely to contain individuals in a wider variety of orientations, which would increase the overall drag force of the swarm. Furthermore, individuals in looser aggregations are more likely to be engaged in feeding activities and so would open their filtering baskets, which further increases levels of drag. For instance, Kils (1981) estimated that krill with open filtering baskets would encounter more than three times the drag force than those with closed filtering baskets when traveling at 10 cm s^{-1} .

Equation 7 shows that the level of drag force increases with velocity to the power 2. We found that the best fit to the observed velocity magnitudes within swarms was

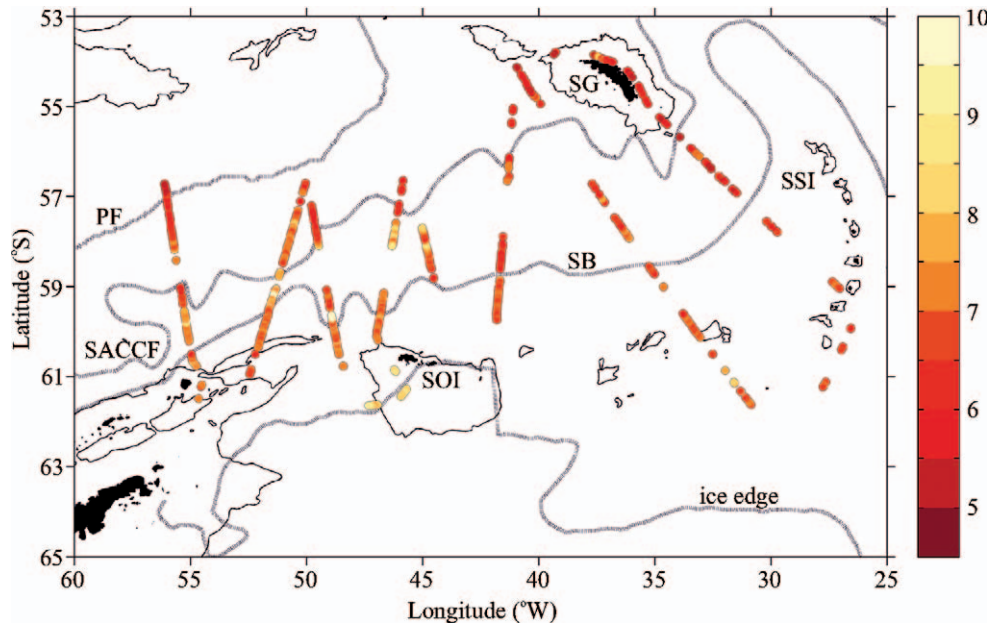


Fig. 7. Predicted net displacement magnitude (m') along the cruise track using Eq. 5. Land masses, fronts, and ice edges as described in Fig. 1; the 1000 m isobath is plotted in black.

achieved through using a linear polynomial function, meaning that swarm speed decreased with increasing velocity to the power 1. This indicates that krill may be acting to decrease drag force or increase swimming effort within higher background velocities. For instance, Kils (1981) posits that increasing flow around the outside of the filtering basket at higher velocities makes the basket more compact, resulting in less water being filtered per unit distance. This effect will decrease C_D with increasing V , so reducing the power relationship between F_D and V to levels below 2. Indeed, the functional relationship between F_D and V derived by Kils (1981) for krill with open filtering baskets was to the power of 1.41.

A further factor that may act to make the power relationship closer to 1 is the means by which velocity magnitudes were measured by the ADCP. Pleuddemann and Pinkel (1989), Heywood (1996), and Tarling et al. (2001) all noted that estimated migration speeds of bands of migrating zooplankton were lower using Doppler shift than tracking vertical displacement of backscatter over time. The explanation offered by Pleuddemann and Pinkel

(1989) was that migrating organisms that cause backscatter are only a proportion of the total backscattering field, of which much is moving at the speed of the background flow. This tends to produce Doppler values less than the true rates of movement. As the proportion of backscattering migrators increases relative to the nonmigrators, the Doppler velocities will approach the true rates of movement. In the case of krill swarms moving more slowly than the background current, the ADCP may overestimate true speed since it will also include measurements of passive particles within the swarms that are traveling at the faster background rate. Conversely, for swarms traveling faster than the background flow, their true speed of motion may be biased low by the ADCP. In terms of the relationship between F_D and V , the true decrease in V resulting from drag force may be masked by the inflated estimate of V derived by the ADCP. The result is that the power relationship would tend toward 1 rather than 2.

Internal and external influences on swarm movement—Net displacement magnitude (m): Best-subset analysis identified

Table 5. Best-fitting regression models constructed from the predictor variables specified in Table 2 and with d as the response variable. The table shows the two best models for each number of predictors up to a maximum of three predictor variables. See Table 4 caption for an explanation of the statistical metrics used for ranking models. The preferred model is indicated by **.

No. of variables	R^2	R^2 (adj)	Cp mallows	S	1	2	3	4	5	6	7	8	9	10	11	12	13
1**	0.4	0.3	7.1	33.418						X							
1	0.3	0.2	8.7	33.432													X
2	0.5	0.4	6.8	33.407						X							X
2	0.5	0.4	6.8	33.407										X			X
3	0.6	0.5	6.2	33.393						X			X				X
3	0.6	0.5	6.4	33.395				X						X			X

1. Log swarm length (m). 2. Log thickness (m). 3. Log area (m²). 4. Log distance to next swarm (m). 5. Log packing concentration (ind. m⁻³). 6. Latitude (°). 7. Distance to coast (km). 8. Bottom depth (m). 9. Distance to ice (km). 10. Temperature (°C). 11. Salinity. 12. PAR ($\mu\text{E m}^{-2} \text{s}^{-1}$). 13. Fluorescence ($\text{mg Chl } a \text{ m}^{-3}$).

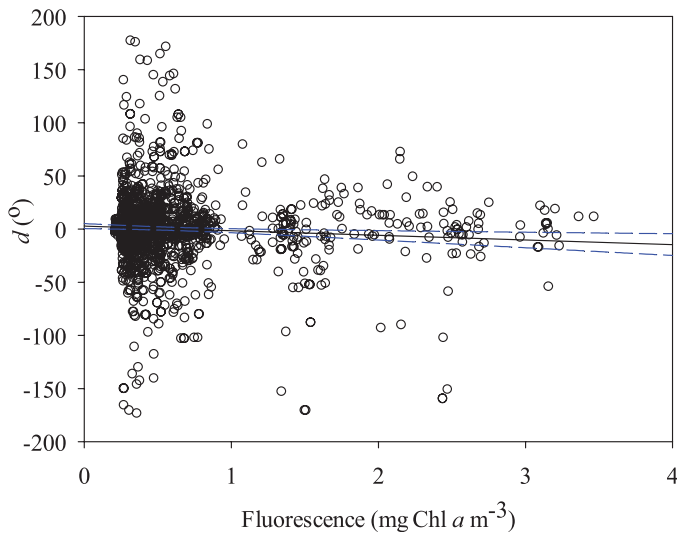


Fig. 8. Linear regression models fitted to d' ($^{\circ}$) as the dependent variable and with fluorescence ($\text{mg Chl } a \text{ m}^{-3}$) as the independent variable, representing the only variable with significant explanatory power. Dashed lines represent 95% confidence intervals.

log swarm area, salinity, and distance to nearest ice as having the greatest significant explanatory powers in accounting for variance in m , with log swarm area having the highest individual explanatory power. m was positive with respect to log swarm area, meaning that the predicted displacement magnitude (m') increased as swarms became larger. Salinity generally decreases from south to north in the present survey. However, in the more southerly latitudes, salinity also declines steeply relative to the proximity of the ice, particularly within 100 km of the ice edge. Swarms in these regions tended to show higher levels of displacement than those farther away from the ice.

Differences in log swarm area accounted for a range of around 4 cm s^{-1} in displacement magnitude, with the smallest swarms predicted to have an average displacement of around 5 cm s^{-1} and the largest, 9 cm s^{-1} . Mauchline (1980) recognized that different krill-swarms may adopt different formations according to their functional attributes, such that aggregations that have located patches of food have different sizes and structures from those that are in the process of searching. This concept has been reinforced by subsequent studies by Antezana and Ray (1983), Hamner et al. (1983), and O'Brien (1987), who noted the adaptive benefits of altering swarm formation according to the balance of internal demands and external forces. In the present instance, swarms with larger areas may be those in a searching mode, as observed by Hamner et al. (1983). In such a mode, it is necessary to move at speeds that differ from those of the prevailing background flow so that new, potentially unexploited bodies of water are encountered. Alternatively, they may show a greater tendency to be in swarms as a response to predators, given laboratory results showing decreases in nearest-neighbor distances when exposed to fish predators (O'Brien and Ritz 1988; Hamner and Hamner 2000).

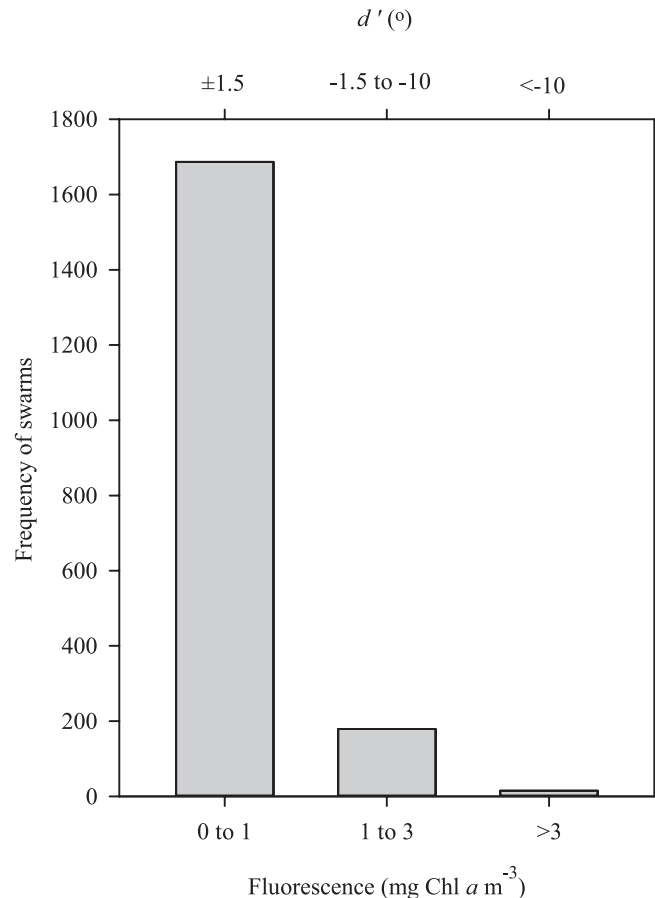


Fig. 9. Distribution of swarms between intervals of fluorescence ($\text{mg Chl } a \text{ m}^{-3}$) and the equivalent values of d' ($^{\circ}$) according to Eq. 6.

Ritz (2000) proposed that an additional benefit to swimming in cohesive groups is that the swimming action generates favorable currents that could be exploited by members to reduce the cost of forward propulsion. For instance, mysid swarms expend three to seven times less energy than small groups of individuals swimming uncohesively. These swarms produce powerful downdrafts that induce an updraft at the margins of the swarm that the mysids may continually move into and out of to their maximum energetic benefit (Ritz et al. 1997). The situation in Antarctic krill swarms is less understood since it has been exceptionally difficult to induce them to school in captivity (Kawaguchi et al. 2010). However, some useful analyses have been performed on individual and small aggregations of specimens from which certain principles can be inferred. For instance, Ebina and Miki (1996), Patria and Wiese (2004), and Catton et al. (2011) found that Antarctic krill produced hydrodynamic disturbances that extended for several body lengths, well within the range of the average nearest-neighbor distance within schools (Catton et al. 2011). Furthermore, Catton et al. (2011) showed that the flow fields of several krill interacted to make a stronger and more persistent hydrodynamic cue as well as a velocity boost to nearest neighbors. It is possible therefore that the

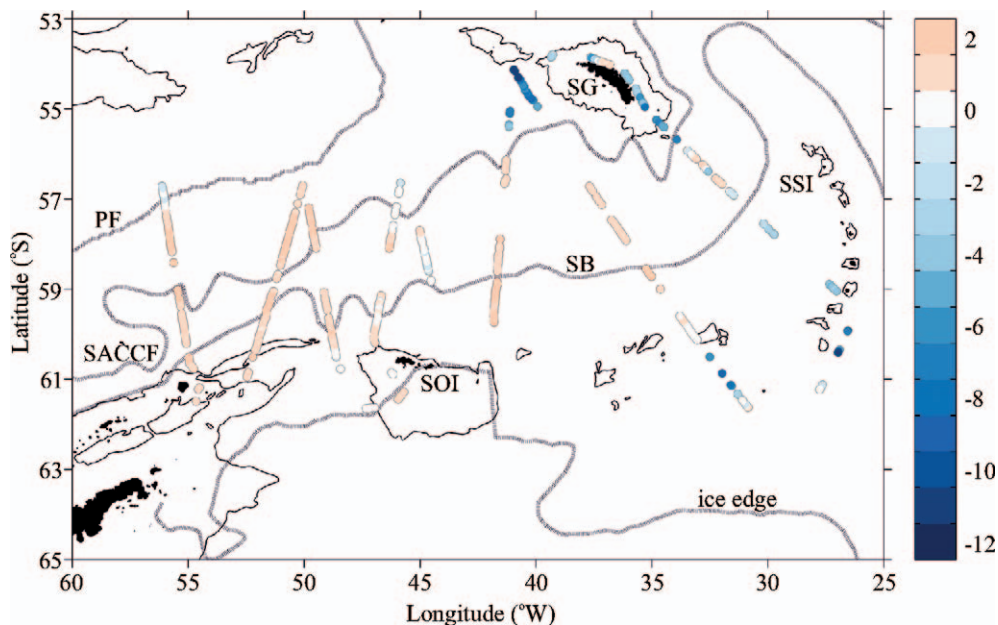


Fig. 10. Predicted net angle of deviation (d') along the cruise track using Eq. 6. Land masses, fronts, and ice edges as described in Fig. 1; the 1000 m isobath is plotted in black. Positive values indicate a predicted counterclockwise deviation from the background flow, negative values a predicted clockwise deviation.

collective speed of krill within swarms may be enhanced through positive interactions of their combined flow fields.

Salinity and distance to nearest ice were identified as also having significant explanatory power toward variance in m . Both parameters had a similar level of influence on the fit of the model to the data, with their relationship to m being negative. In effect, for swarms of similar sizes, the tendency would be for them to become more displaced from the background flow when in the vicinity of ice or in low-salinity regions. The greater displacement may be a result of the krill becoming more active in trying to avoid advection out of this environment.

The ice edge is recognized as a beneficial environment for krill in terms of its link to productivity and as a suitable refuge for early developmental stages (Kawaguchi et al. 1986; Daly and Macaulay 1988). Autonomous underwater vehicle transects revealed an increase in krill concentration within a narrow band along the ice edge (Brierley et al. 2002). Salinity decreases in the vicinity of the ice edge and may even provide the cue by which krill detect the ice edge and alter their patterns of movement. Although a response to such a cue has yet to be identified in krill, it is not unprecedented in crustaceans given that the blue crab *Callinectes sapidus* alters its ascent rate in the water column on the basis of its detection of the rate of salinity increase during rising tides (Forward et al. 1995). Relatively low salinities were also observed in the vicinity of South Georgia, probably as a result of glacial runoff. This is a region of raised productivity that has also been shown to improve krill performance (Atkinson et al. 2006). As with the ice edge, increased levels of displacement from the prevailing flows may be a strategy to avoid being moved away from favorable conditions.

Conversely, high-salinity regions were observed at mid-latitudes and toward the southwestern part of the cruise path, close to the Antarctic Peninsula, in the source region of the Weddell–Scotia Confluence (Gordon et al. 1977; Patterson and Sievers 1980). The Antarctic Peninsula has been identified as one of the main origins of much of the krill found in the Scotia Sea (Hofmann et al. 1998). Prevailing flows in this region are generally to the northeast and physical models have demonstrated that passive particles released in these regions are moved into the Scotia Sea and toward South Georgia (Thorpe et al. 2004). Our prediction that krill swarms show less displacement in this region supports the view of swarms moving with the prevailing flows and being exported into the Scotia Sea.

Net direction of swarm movement (d): Fluorescence was identified as being the only parameter to have a significant explanatory power toward d . The majority of swarms were found at fluorescence levels less than $1 \text{ mg Chl } a \text{ m}^{-3}$ where there was little deviation ($\pm 1.5^\circ$) from the direction of the background flow. However, swarms found at higher fluorescence levels showed increasing deviation, becoming greater than 10° at the highest fluorescence levels. Where high levels of deviation were predicted, this was in a clockwise direction relative to the background flow.

A pattern of increased turning at high food concentrations has been previously reported in a mesocosm study carried out on the euphausiid *Thysaneosira raschii* by Price (1989). The krill were maintained in a tower tank that was 10.5 m deep, 3.7 m in diameter, and held 117 m^3 of water. Two-hundred adult krill were introduced and, after some control experiments, a 2.5 m^3 patch of concentrated diatoms was introduced. Krill density within the patch was an order of magnitude higher than the control density within 30 min

after algal introduction. Orientation of the swimming paths became more horizontal, swimming speed doubled, and sinking bouts were almost entirely eliminated inside the algal patch. Individual krill kept themselves within the patch by turning back at the boundary so that the angle of approach to and return from the edge was held roughly constant.

There is a lack of studies on the feeding behavior within such large mesocosms in *Euphausia superba*, although feeding responses within tanks have been reported. Strand and Hamner (1990), for instance, managed to induce schooling behavior in *E. superba* maintained in circular tanks of 1.75 m diameter and 1 m depth and then examined the responses of these schools to visual and chemical stimuli, including concentrated diatoms. They observed that individuals slowed and began feeding on encountering a small 100 mL patch of the food. The addition of several liters of concentrated diatoms to the tank caused a reduction of swimming speed and increased feeding activity and the krill often stopped schooling.

A simple response to food stimuli such as increased instantaneous turning angles can have much larger consequences to distributional patterns. For instance, Cresswell et al. (2007) implemented an individual-based model where krill were able to change their swimming speed and turn rate when encountering areas with higher-than-average chlorophyll within a region of low potential predation rate. The model showed that such behavior could improve the ability of krill to remain within favorable regions. When parameterized for the South Georgia region, the model krill concentrated at the shelf-break region, which corresponds well with observations (Witek et al. 1981; Trathan et al. 1998).

Wider context—The manner in which ADCPs integrate all particles within depth–time bins means that they are likely to underestimate the deviation of krill swarm movement from the speed and direction of background flows. Therefore, there must be some caution in applying the parameterizations within this study to predictive tracking models. Furthermore, this study only considered movement patterns discerned at the instant that the swarm was observed and did not involve subsequent tracking of the swarms to determine if such movements are reflective of the longer-term trajectories of these swarms. Nevertheless, we believe that the fact that these measurements were made on over 4000 swarms over a large area of the Scotia Sea gives us scope to generalize both in terms of what may be considered to be average patterns across all swarms and how these patterns of movement may be scaled up from the individual swarm-level to population-level patterns. Furthermore, through carrying out such a large-scale analysis, the present study was able to identify physical forces acting on swarms, such as drag, as well as the differing tendencies in swarm movement patterns in different contexts. Future research will examine some of the consequences of these instantaneous patterns of movement in terms of distribution of swarms within the flow fields of the Scotia Sea.

Acknowledgments

We thank the crew and scientists aboard the R/V *James Clark Ross* during the cruise JR82 for their assistance in collecting

biological and oceanographic data. We also thank Doug Bone for assembling and maintaining the net gear and Nathan Cunningham for organizing and retrieving data. Sophie Fielding and Thor Klevjer assisted in the acoustic identification of krill swarms, as reported in previously published works. Angus Atkinson, David Pond, and Rachel Shreeve helped with the morphometric measurement and maturity staging of Antarctic krill captured by nets during the cruise, and Mike Meredith gave advice on the ADCP data. To visualize our data, we have made use of color palettes devised by C. Brewer and M. Niccoli. We are grateful to the editor and two reviewers for helpful comments that improved this study.

This work was carried out as part of the Ecosystems program at the British Antarctic Survey, Natural Environment Research Council.

References

- ANTEZANA, T., AND K. RAY. 1983. Aggregation of *Euphausia superba* as an adaptive group strategy to the Antarctic ecosystem. *Ber. Polarforsch.* **4**: 199–215.
- ATKINSON, A., V. SIEGEL, E. PAKHOMOV, AND P. ROTHERY. 2004. Long-term decline in krill stock and increase in salps within the Southern Ocean. *Nature* **432**: 100–103, doi:10.1038/nature02996
- , AND OTHERS. 2006. Natural growth rates in Antarctic krill (*Euphausia superba*): II. Predictive models based on food, temperature, body length, sex, and maturity stage. *Limnol. Oceanogr.* **51**: 973–987, doi:10.4319/lo.2006.51.2.0973
- , AND ———. 2008. Oceanic circumpolar habitats of Antarctic krill. *Mar. Ecol. Prog. Ser.* **362**: 1–23, doi:10.3354/meps07498
- BRIERLEY, A. S., AND M. J. COX. 2010. Shapes of krill swarms and fish schools emerge as aggregation members avoid predators and access oxygen. *Curr. Biol.* **20**: 1758–1762, doi:10.1016/j.cub.2010.08.041
- , AND OTHERS. 2002. Antarctic krill under sea ice: Elevated abundance in a narrow band just south of ice edge. *Science* **295**: 1890–1892, doi:10.1126/science.1068574
- CATTON, K. B., D. R. WEBSTER, S. KAWAGUCHI, AND J. YEN. 2011. The hydrodynamic disturbances of two species of krill: Implications for aggregation structure. *J. Exp. Biol.* **214**: 1845–1856, doi:10.1242/jeb.050997
- CCAMLR. 2005. Report of the first meeting of the subgroup on acoustic survey and analysis methods SC-CCAMLR-XXIV/BG/3.
- CLARKE, A., AND D. J. MORRIS. 1983. Towards an energy budget for krill: The physiology and biochemistry of *Euphausia superba* Dana. *Polar Biol.* **2**: 69–86, doi:10.1007/BF00303172
- COETZEE, J. 2000. Use of a shoal analysis and patch estimation system (SHAPES) to characterize sardine schools. *Aquat. Living Resour.* **13**: 1–10, doi:10.1016/S0990-7440(00)00139-X
- COMISO, J. 2000 (updated 2012). Bootstrap sea ice concentrations from Nimbus-7 SMMR and DMSP SSM/I-SSMIS Version 2. Boulder, Colorado: NASA DAAC at the National Snow and Ice Data Center.
- CONTI, S. G., AND D. A. DEMER. 2006. Improved parameterization of the SDWBA for estimating krill target strength. *ICES J. Mar. Sci.* **63**: 928–935, doi:10.1016/j.icesjms.2006.02.007
- CRESSWELL, K. A., G. A. TARLING, AND M. T. BURROWS. 2007. Behavior affects local-scale distributions of Antarctic krill around South Georgia. *Mar. Ecol. Prog. Ser.* **343**: 193–206, doi:10.3354/meps06908

- CUNNINGHAM, S., AND M. PAVIC. 2007. Surface geostrophic currents across the Antarctic circumpolar current in Drake Passage from 1992 to 2004. *Prog. Oceanogr.* **73**: 292–310, doi:10.1016/j.pocean.2006.07.010
- DALY, K. L., AND M. C. MACAULAY. 1988. Abundance and distribution of krill in the ice edge zone of the Weddell Sea, austral spring 1983. *Deep-Sea Res. I* **35**: 21–41, doi:10.1016/0198-0149(88)90055-6
- DEMER, D. A., M. BARANGE, AND A. J. BOYD. 2000. Measurements of three-dimensional fish school velocities with an acoustic Doppler current profiler. *Fish. Res.* **47**: 201–214, doi:10.1016/S0165-7836(00)00170-3
- , AND S. G. CONTI. 2003. Validation of the stochastic distorted-wave Born approximation model with broad bandwidth total target strength measurements of Antarctic krill. *ICES J. Mar. Sci.* **60**: 625–635, doi:10.1016/S1054-3139(03)00063-8
- EBINA, Y., AND T. MIKI. 1995. Range and biological significance of characteristic water currents produced by the shrimps *Euphausia superba* and *Metapenaeus intermedius*. *Zoology (Jena)* **99**: 163–174.
- FACH, B. A., AND J. M. KLINCK. 2006. Transport of Antarctic krill (*Euphausia superba*) across the Scotia Sea. Part I: Circulation and particle tracking simulations. *Deep-Sea Res. I* **53**: 987–1010, doi:10.1016/j.dsr.2006.03.006
- FLAGG, C. N., AND S. L. SMITH. 1989. On the use of acoustic Doppler current profiler to measure zooplankton abundance. *Deep Sea Res.* **36**: 455–474, doi:10.1016/0198-0149(89)90047-2
- FORWARD, R. B., R. A. TANKERSLEY, M. C. DEVRIES, AND D. RITTSCHOF. 1995. Sensory physiology and behavior of blue crab (*Callinectes sapidus*) postlarvae during horizontal transport. *Mar. Freshw. Behav. Phys.* **26**: 233–248, doi:10.1080/10236249509378942
- FOSTER, E. G., D. A. RITZ, J. E. OSBORN, AND K. M. SWADLING. 2001. Schooling affects the feeding success of Australian salmon (*Arripis trutta*) when preying on mysid swarms (*Paramesopodopsis rufa*). *J. Exp. Mar. Biol. Ecol.* **261**: 93–106, doi:10.1016/S0022-0981(01)00265-9
- GORDON, A. L., D. T. GEORGI, AND H. W. TAYLOR. 1977. Antarctic Polar Front Zone in western Scotia Sea—summer 1975. *J. Phys. Oceanogr.* **7**: 309–328, doi:10.1175/1520-0485(1977)007<0309:APFZIT>2.0.CO;2
- GRUNBAUM, D. 1998. Schooling as a strategy for taxis in a noisy environment. *Evol. Ecol.* **12**: 503–522, doi:10.1023/A:1006574607845
- HAMNER, W. M. 1984. Aspects of schooling of *Euphausia superba*. *J. Crustacean Biol.* **4**, (Special Issue), 67–74.
- , AND P. P. HAMNER. 2000. Behavior of Antarctic krill (*Euphausia superba*): Schooling, foraging, and antipredatory behavior. *Can. J. Fish. Aquat. Sci.* **57**: 192–202, doi:10.1139/f00-195
- , ———, S. W. STRAND, AND R. W. GILMER. 1983. Behavior of Antarctic krill *Euphausia superba*: Chemoreception, feeding, schooling and molting. *Science* **220**: 433–435, doi:10.1126/science.220.4595.433
- HARDY, A. C., AND E. R. GUNTHER. 1935. The plankton of the South Georgia whaling grounds and adjacent waters, 1926–1927. *Discov. Rep.* **11**: 1–456.
- HEWITT, R. P., AND OTHERS. 2004. Biomass of Antarctic krill in the Scotia Sea in January/February 2000 and its use in revising an estimate of precautionary yield. *Deep-Sea Res. II* **51**: 1215–1236, doi:10.1016/j.dsr2.2004.06.011
- HEYWOOD, K. J. 1996. Diel vertical migration of zooplankton in the Northeast Atlantic. *J. Plankt. Res.* **18**: 163–184, doi:10.1093/plankt/18.2.163
- HILL, S. L., P. N. TRATHAN, AND D. J. AGNEW. 2009. The risk to fishery performance associated with spatially resolved management of Antarctic krill (*Euphausia superba*) harvesting. *ICES J. Mar. Sci.* **66**: 2148–2154, doi:10.1093/icesjms/fsp172
- HOFMANN, E. E., J. M. KLINCK, R. A. LOCARNINI, B. FACH, AND E. MURPHY. 1998. Krill transport in the Scotia Sea and environs. *Antarct. Sci.* **10**: 406–415, doi:10.1017/S0954102098000492
- KAWAGUCHI, K., O. MATSUDA, S. ISHIKAWA, AND Y. NAITO. 1986. A light trap to collect krill and other micronektonic and planktonic animals under the Antarctic coastal fast ice. *Polar Biol.* **6**: 37–42, doi:10.1007/BF00446238
- KAWAGUCHI, S., R. KING, R. MEIJERS, J. E. OSBORN, K. M. SWADLING, D. A. RITZ, AND S. NICOL. 2010. An experimental aquarium for observing the schooling behavior of Antarctic krill (*Euphausia superba*). *Deep-Sea Res. II* **57**: 683–692, doi:10.1016/j.dsr2.2009.10.017
- KILS, U. 1979. Swimming speed and escape capacity of Antarctic krill, *Euphausia superba*. *Meeresforschung* **27**: 264–266.
- . 1981. Swimming behavior, swimming performance and energy balance of Antarctic krill *Euphausia superba*. *BIO-MASS Sci. Ser.* **3**: 1–121.
- LAWSON, G. L., P. H. WIEBE, T. K. STANTON, AND C. J. ASHJIAN. 2008. Euphausiid distribution along the Western Antarctic Peninsula—part A: Development of robust multi-frequency acoustic techniques to identify euphausiid aggregations and quantify euphausiid size, abundance and biomass. *Deep-Sea Res. II* **55**: 412–431, doi:10.1016/j.dsr2.2007.11.010
- MARR, J. W. S. 1962. The natural history and geography of the Antarctic krill. *Discov. Rep.* **32**: 33–464.
- MAUCLINE, J. 1980. Studies on patches of krill *Euphausia superba* Dana. *Biomass Handb. Ser.* **6**.
- MCGEHEE, D. E., R. L. O'DRISCOLL, AND L. V. M. TRAYKOVSKI. 1998. Effects of orientation on acoustic scattering from Antarctic krill at 120 kHz. *Deep-Sea Res. II* **45**: 1273–1294, doi:10.1016/S0967-0645(98)00036-8
- MCMANUS, M. A., AND C. B. WOODSON. 2012. Plankton distribution and ocean dispersal. *J. Exp. Biol.* **215**: 1008–1016, doi:10.1242/jeb.059014
- MOORE, J. K., M. R. ABBOTT, AND J. G. RICHMAN. 1999. Location and dynamics of the Antarctic Polar Front from satellite sea surface temperature data. *J. Geophys. Res. (C Oceans)* **104**: 3059–3073, doi:10.1029/1998JC900032
- NOWACEK, D. P., AND OTHERS. 2011. Super-aggregations of krill and Humpback whales in Wilhelmina Bay, Antarctic Peninsula. *Plos One* **6**: e19173, doi:10.1371/journal.pone.0019173
- O'BRIEN, D. P. 1987. Description of escape responses of krill (Crustacea, Euphausiacea), with particular reference to swarming behavior and the size and proximity of the predator. *J. Crust. Biol.* **7**: 449–457, doi:10.2307/1548294
- , AND D. A. RITZ. 1988. Escape responses of gregarious mysids (Crustacea, Mysidacea)—towards a general classification of escape responses in aggregated crustaceans. *J. Exp. Mar. Biol. Ecol.* **116**: 257–272, doi:10.1016/0022-0981(88)90031-7
- ORSI, A. H., T. WHITWORTH, AND W. D. NOWLIN. 1995. On the meridional extent and fronts of the Antarctic Circumpolar Current. *Deep-Sea Res. I* **42**: 641–673, doi:10.1016/0967-0637(95)00021-W
- PATRIA, M. P., AND K. WIESE. 2004. Swimming in formation in krill (Euphausiacea), a hypothesis: Dynamics of the flow field, properties of antennular sensor systems and a sensory-motor link. *J. Plankt. Res.* **26**: 1315–1325, doi:10.1093/plankt/fbh122
- PATTERSON, S. L., AND H. A. SIEVERS. 1980. The Weddell–Scotia confluence. *J. Phys. Oceanogr.* **10**: 1584–1610, doi:10.1175/1520-0485(1980)010<1584:TWSC>2.0.CO;2

- PLEUDEMANN, A. J., AND R. PINKEL. 1989. Characterization of the patterns of diel migration using a Doppler sonar. *Deep-Sea Res.* **36**: 509–530.
- PRICE, H. J. 1989. Swimming behavior of krill in response to algal patches—a mesocosm study. *Limnol. Oceanogr.* **34**: 649–659, doi:10.4319/lo.1989.34.4.0649
- RITZ, D. A. 2000. Is social aggregation in aquatic crustaceans a strategy to conserve energy? *Can. J. Fish. Aquat. Sci.* **57**: 59–67, doi:10.1139/f00-170
- , A. J. HOBDA, J. C. MONTGOMERY, AND A. J. W. WARD. 2011. Social aggregation in the pelagic zone with special reference to fish and invertebrates. *Adv. Mar. Biol.* **60**: 161–227, doi:10.1016/B978-0-12-385529-9.00004-4
- , J. E. OSBORN, AND A. E. J. OCKEN. 1997. Influence of food and predatory attack on mysid swarm dynamics. *J. Mar. Biol. Assoc. U.K.* **77**: 31–42, doi:10.1017/S0025315400033762
- SMITH, I. J., D. P. STEVENS, K. J. HEYWOOD, AND M. P. MEREDITH. 2010. The flow of the Antarctic Circumpolar Current over the North Scotia Ridge. *Deep Sea Res. I* **57**: 14–28, doi:10.1016/j.dsr.2009.10.010
- STRAND, S. W., AND W. M. HAMNER. 1990. Schooling behavior of Antarctic krill (*Euphausia superba*) in laboratory aquariums—reactions to chemical and visual stimuli. *Mar. Biol.* **106**: 355–359, doi:10.1007/BF01344312
- SWADLING, K. M., D. A. RITZ, S. NICOL, J. E. OSBORN, AND L. J. GURNEY. 2005. Respiration rate and cost of swimming for Antarctic krill, *Euphausia superba*, in large groups in the laboratory. *Mar. Biol.* **146**: 1169–1175, doi:10.1007/s00227-004-1519-z
- TARLING, G. A. 2003. Sex dependent diel vertical migration in Northern krill and its consequences for population dynamics. *Mar. Ecol. Prog. Ser.* **260**: 173–188, doi:10.3354/meps260173
- , J. CUZIN-ROUDY, AND F. BUCHHOLZ. 1999. Vertical migration behavior in the northern krill *Meganctiphanes norvegica* is influenced by moult and reproductive processes. *Mar. Ecol. Prog. Ser.* **190**: 253–262, doi:10.3354/meps190253
- , J. B. L. MATTHEWS, P. DAVID, O. GUERIN, AND F. BUCHHOLZ. 2001. The swarm dynamics of northern krill (*Meganctiphanes norvegica*) and pteropods (*Cavolinia inflexa*) during vertical migration in the Ligurian Sea observed by an acoustic Doppler current profiler. *Deep-Sea Res. I* **48**: 1671–1686, doi:10.1016/S0967-0637(00)00105-9
- , AND OTHERS. 2009. Variability and predictability of Antarctic krill swarm structure. *Deep-Sea Res. I* **56**: 1994–2012, doi:10.1016/j.dsr.2009.07.004
- THORPE, S. E., K. J. HEYWOOD, M. A. BRANDON, AND D. P. STEVENS. 2002. Variability of the southern Antarctic Circumpolar Current front north of South Georgia. *J. Mar. Sys.* **37**: 87–105, doi:10.1016/S0924-7963(02)00197-5
- , ———, D. P. STEVENS, AND M. A. BRANDON. 2004. Tracking passive drifters in a high resolution ocean model: Implications for interannual variability of larval krill transport to South Georgia. *Deep-Sea Res. I* **51**: 909–920, doi:10.1016/j.dsr.2004.02.008
- , E. J. MURPHY, AND J. L. WATKINS. 2007. Circumpolar connections between Antarctic krill (*Euphausia superba* Dana) populations: Investigating the roles of ocean and sea ice transport. *Deep-Sea Res. I* **54**: 792–810, doi:10.1016/j.dsr.2007.01.008
- TRATHAN, P. N., E. J. MURPHY, J. P. CROXALL, AND I. EVERSON. 1998. Use of at-sea distribution data to derive potential foraging ranges of macaroni penguins during the breeding season. *Mar. Ecol. Prog. Ser.* **169**: 263–275, doi:10.3354/meps169263
- WARD, P., AND OTHERS. 2012. Food web structure and bioregions in the Scotia Sea: A seasonal synthesis. *Deep-Sea Res. II* **59–60**: 253–266, doi:10.1016/j.dsr2.2011.08.005
- WATKINS, J. L., AND A. S. BRIERLY. 1996. A post processing technique to remove background noise from echo-integration data. *J. Mar. Sci.* **53**: 339–344.
- , AND A. W. A. MURRAY. 1998. Layers of Antarctic krill, *Euphausia superba*: Are they just long krill swarms? *Mar. Biol.* **131**: 237–247, doi:10.1007/s002270050316
- WITEK, Z., A. KALINOWSKI, A. GRELOWSKI, AND N. WOLNOMIEJSKI. 1981. Studies of aggregations of krill (*Euphausia superba*). *Meeresforsch.* **28**: 228–243.
- YEN, J., J. BROWN, AND D. R. WEBSTER. 2003. Analysis of the flow field of the krill, *Euphausia pacifica*. *Mar. Freshw. Behav. Phy.* **36**: 307–319, doi:10.1080/10236240310001614439
- ZHOU, M., AND R. D. DORLAND. 2004. Aggregation and vertical migration behavior of *Euphausia superba*. *Deep-Sea Res. II* **51**: 2119–2137, doi:10.1016/j.dsr2.2004.07.009

Associate editor: James J. Leichter

Received: 10 July 2013
 Accepted: 26 November 2013
 Amended: 09 January 2014